Editors' Suggestion

Nonequilibrium Response for Markov Jump Processes: Exact Results and Tight Bounds

Timur Aslyamov* and Massimiliano Esposito†
Department of Physics and Materials Science, University of Luxembourg, L-1511 Luxembourg City, Luxembourg

(Received 16 August 2023; revised 13 October 2023; accepted 14 December 2023; published 16 January 2024)

Generalizing response theory of open systems far from equilibrium is a central quest of nonequilibrium statistical physics. Using stochastic thermodynamics, we develop an algebraic method to study the static response of nonequilibrium steady state to arbitrary perturbations. This allows us to derive explicit expressions for the response of edge currents as well as traffic to perturbations in kinetic barriers and driving forces. We also show that these responses satisfy very simple bounds. For the response to energy perturbations, we straightforwardly recover results obtained using nontrivial graph-theoretical methods.

DOI: 10.1103/PhysRevLett.132.037101

Introduction.—Linear response theory is a central tenet in statistical physics [1–3]. The response of systems in steady state at, or close to, equilibrium is described by the seminal fluctuation-dissipation relation [4,5]. Generalizations to study the response of systems in nonequilibrium steady state are a more recent endeavor, in particular since the advent of stochastic thermodynamics [6–16]. Understanding the response of far-from-equilibrium systems is of great conceptual but also practical importance (e.g., to characterize homeostasis, design resilient nanotechnologies, detect critical transitions, and for metabolic control). Progress in this direction relies on our ability to derive useful expressions for static responses, and possibly derive practically meaningful bounds for them.

In this Letter, we study the static response of Markov jump processes within stochastic thermodynamics. In this context, Ref. [17] constitute a frontier. The authors studied the response to perturbations of the energy landscape parameters. They derived an exact result and two bounds using graph-theoretic methods, which can be quite tedious and nonintuitive to use [18–20]. We develop a novel approach based on simple linear algebra, which allows us to go significantly further than currently known results. We first derive a simple and elegant expression for the static response to arbitrary perturbations. We use it to straightforwardly reproduce the main result [17] for the static response to perturbations of the energy landscape. But more importantly we also use it to derive novel and simple expressions for the response of edge currents and traffic to kinetic barriers and driving forces perturbations. We furthermore derive four remarkably simple bounds for these four quantities (see Table I), which can be added to the list of simple bounds valid far-from-equilibrium, together with thermodynamic uncertainty relations [21,22] and speed limits [23].

Setup.—We consider a Markov jump process over a discrete set of N states. Transitions between these states are described by the rate matrix $\mathbb{W}/\tau$, where the element $W_{nm}/\tau \geq 0$ defines the probability per unit time τ to jump from state m to state n. Below we choose $\tau = 1$, to adimensionalize the matrix $\mathbb{W}$. The diagonal elements are defined as $W_{ii} = -\sum_{j\neq i} W_{ij}$. We assume that all transitions are reversible, i.e., $W_{ij} \neq 0$ only if $W_{ji} \neq 0$ and that the matrix $\mathbb{W}$ is irreducible [24]. This ensures the existence of a unique steady-state probability $\boldsymbol{\pi} = (\pi_1, \ldots, \pi_N)^\intercal$ satisfying

$$\mathbb{W} \cdot \boldsymbol{\pi} = \mathbf{0}, \tag{1}$$

where $\sum_{i=1}^N \pi_i = 1$. When the rates depend on a model parameter η, one can define the static response of the nonequilibrium state as $\partial_\eta q$ for an arbitrary quantity q. We also define the sensitivity as $\partial_\eta \ln q \equiv q^{-1}\partial_\eta q$ to ensure that it remains well defined when q becomes negative.

General theory.—The rate matrix $\mathbb{W}$ in Eq. (1) has only one zero eigenvalue [24]. This allows us to rewrite Eq. (1) as

$$\mathbb{K}_n \cdot \boldsymbol{\pi} = \boldsymbol{e}_n, \tag{2a}$$

$$\mathbb{K}_n = \begin{array}{c} 1 \\ \vdots \\ n-1 \\ n \\ n+1 \\ \vdots \\ N \end{array} \begin{pmatrix} W_{11} & W_{12} & \ldots & W_{1N} \\ \vdots & \vdots & \ldots & \vdots \\ W_{n-1,1} & W_{n-1,2} & \ldots & W_{n-1,N} \\ 1 & 1 & \ldots & 1 \\ W_{n+1,1} & W_{n+1,2} & \ldots & W_{n+1,N} \\ \vdots & \vdots & \ldots & \vdots \\ W_{N1} & W_{N2} & \ldots & W_{NN} \end{pmatrix}, \tag{2b}$$

TABLE I. The central and right columns correspond to the response of the current and traffic, respectively. The central and bottom rows are perturbations of the symmetric and antisymmetric edge parameters, respectively.

Control	Current, J_{nm}	Traffic, τ_{nm}
B_{nm}	$-1 \le (\partial \ln J_{nm}/\partial B_{nm}) \le 0$	$-2 \le (\partial \ln \tau_{nm}/\partial B_{nm}) \le 0$
F_{nm}	$0 \le (2/\tau_{nm})(\partial J_{nm}/\partial F_{nm}) \le 1$	$-1 \le (\partial \ln \tau_{nm}/\partial F_{nm}) \le 1$

where $\boldsymbol{e}_n$ denotes the vector with a 1 for the nth element and 0's elsewhere, and where the matrix $\mathbb{K}_n$ coincides with the rate-matrix $\mathbb{W}$ except the nth row. Since $\mathbb{W}$ is irreducible, it has a single zero eigenvalue and $N-1$ nonzero ones with $\mathrm{Re}\,\lambda_i < 0$. In Appendix A, we show that the determinant of $\mathbb{K}_n$ can be expressed in terms of the nonzero eigenvalues of $\mathbb{W}$ (see also Ref. [25]):

$$D = \det \mathbb{K}_n = \prod_{i=1}^{N-1} \lambda_i \neq 0. \tag{3}$$

Despite the fact that the matrix $\mathbb{K}_n$ depends on the choice of index n, its determinant $D = \det \mathbb{K}_n$ does not [see Eq. (3)]. Since $D \neq 0$, $\mathbb{K}_n$ is invertible and we can solve Eq. (2a):

$$\boldsymbol{\pi} = \mathbb{K}_n^{-1} \cdot \boldsymbol{e}_n. \tag{4}$$

To find the linear response $\partial_\eta \boldsymbol{\pi}$ we calculate the derivative ∂_η of Eq. (2a), $\partial_\eta[\mathbb{K}_n(\eta) \cdot \boldsymbol{\pi}(\eta)] = \boldsymbol{0}$, and get

$$\mathbb{K}_n \cdot \partial_\eta \boldsymbol{\pi} = -\partial_\eta \mathbb{K}_n \cdot \boldsymbol{\pi}. \tag{5}$$

Solving Eq. (5), we arrive at the desired result:

$$\partial_\eta \boldsymbol{\pi} = -\mathbb{K}_n^{-1} \cdot \partial_\eta \mathbb{K}_n \cdot \boldsymbol{\pi}. \tag{6}$$

Equation (6) will be central in what follows. Indeed, it provides a linear algebra-based method to calculate different nonequilibrium responses, which is much simpler and direct than methods based on graph theory representations of $\boldsymbol{\pi}$. At this stage, Eq. (6) holds for any dependence of $\mathbb{W}(\eta)$ on the control parameter.

Rate-matrix model.—To proceed, we follow Ref. [17] and parametrize the nondiagonal elements of the rate matrix as

$$W_{ij} = \mathrm{e}^{-(B_{ij} - E_j - F_{ij}/2)}, \tag{7}$$

where E_j are the vertex parameters, $B_{ij} = B_{ji}$ are the symmetric edge parameters, and $F_{ij} = -F_{ji}$ are the antisymmetric edge parameters. Equation (7) is reminiscent of Arrhenius rates that characterize the transition rates of a system in an energy landscape with wells with bottom energy E_j, connected to other wells via barriers of heights B_{ij}, and subjected to nonconservative driving forces F_{ij} along the transition paths [26]. These rates satisfy local detailed balance ensuring the compatibility with stochastic thermodynamics [26–28].

Vertex parameters.—To calculate $\partial_{E_n} \boldsymbol{\pi}$, we note that only the nth column of the matrix $\mathbb{K}_n$ depends on E_n. Therefore,

$$\partial_{E_n} \mathbb{K}_n = \begin{array}{c} \\ 1 \\ \vdots \\ n-1 \\ n \\ n+1 \\ \vdots \\ N \end{array} \begin{array}{c} n \\ \left(\begin{array}{ccc} & W_{1,n} & \\ & \vdots & \\ & W_{n-1,n} & \\ & 0 & \\ & W_{n-1,n} & \\ & \vdots & \\ & W_{N,n} & \end{array} \right) \end{array}, \tag{8}$$

where all columns but the nth one are zero. The element (n, n) is zero because $K_{n,n} = 1$. Here and below, empty spaces in matrices denote zeros. Inserting Eq. (8) into Eq. (6), we immediately recover a key result of Ref. [17] obtained using nontrivial graph-theoretical methods, namely

$$\partial_{E_n} \boldsymbol{\pi} = -\pi_n \mathbb{K}_n^{-1} \cdot (\boldsymbol{K}_n - \boldsymbol{e}_n) = -\pi_n(\boldsymbol{e}_n - \boldsymbol{\pi}), \tag{9}$$

where $\boldsymbol{K}_n$ is the nth column of $\mathbb{K}_n$ and where we used Eq. (4).

Symmetric edge parameters.—We proceed with calculating $\partial_{B_{nm}} \boldsymbol{\pi}$. One can see from Eq. (7) that such a perturbation changes W_{nm} and W_{mn}. These rates are also contained in the diagonal elements of the matrix $\mathbb{W}$ since $W_{nn} = -\sum_{m \neq n} W_{mn}$. Overall four elements depend on B_{nm}: W_{nm}, W_{nn}, W_{mn}, and W_{mm}. But the matrix $\mathbb{K}_n$ defined in Eq. (2b) only contains two of those elements because the nth row is made of ones ($K_{nm} = 1$ and $K_{nn} = 1$). This is why matrix $\mathbb{K}_n$ is convenient to study the perturbations of the edge (n, m). Using Eq. (7), their derivatives reads $\partial_{B_{nm}} W_{mn} = -W_{mn}$ and $\partial_{B_{nm}} W_{mm} = -\partial_{B_{nm}} W_{nm} = W_{nm}$, and we find that

$$\partial_{B_{nm}}\mathbb{K}_n = \begin{array}{c} \\ 1 \\ \vdots \\ m \\ \vdots \\ N \end{array}\begin{array}{c} \begin{array}{ccccccc} 1 & \dots & n & \dots & m & \dots & N \end{array} \\ \left(\begin{array}{ccccccc} & & & & & & \\ & & & & & & \\ & & -W_{mn} & & W_{nm} & & \\ & & & & & & \\ & & & & & & \end{array} \right) \end{array}. \quad (10)$$

Calculating $(\partial_{B_{nm}}\mathbb{K}_n)\cdot\boldsymbol{\pi}$ and inserting into Eq. (6) we get

$$\partial_{B_{nm}}\boldsymbol{\pi} = -\mathbb{K}_n^{-1}\cdot \boldsymbol{e}_m(W_{nm}\pi_m - W_{mn}\pi_n) = -\frac{\boldsymbol{\kappa}^{nm}}{D}J_{nm}, \quad (11)$$

where we recognize the current $J_{nm} = W_{nm}\pi_m - W_{mn}\pi_n$ from m to n, and where $\boldsymbol{\kappa}^{nm}/D$ is the vector with the elements from the mth column of the matrix $\mathbb{K}_n^{-1}$. Below we abuse notation for the vector $\boldsymbol{\kappa} = \boldsymbol{\kappa}^{nm}$, which depends on the choice of the indexes n and m. The elements κ_i can be defined in terms of the minors $M_{im}(\mathbb{K}_n^\intercal)$ of the matrix $\mathbb{K}_n^\intercal$:

$$\kappa_i = (-1)^{i+m}M_{im}(\mathbb{K}_n^\intercal) = (-1)^{i+m}M_{mi}(\mathbb{K}_n). \quad (12)$$

Since the minors $M_{mi}(\mathbb{K}_n)$ do not include the mth row of the matrix $\mathbb{K}_n$, the elements κ_i do not depend on B_{nm} and F_{nm} [see Eq. (2b)].

Equation (11) is a new result. In Ref. [17], only the following bound was obtained: $|\partial_{B_{nm}}\pi_i| \le \pi_i(1-\pi_i)\tanh(F_{\max}/4)$, where $F_{\max}$ is the maximum absolute value of the affinity along all cycles containing the edge (n, m). A numerical comparison between the two is given in Appendix B; see Fig. 1. A direct implication of our result is that the response is suppressed, $\partial_{B_{nm}}\boldsymbol{\pi} = 0$, when the edge (n, m) is detailed balanced $J_{nm} = 0$. Instead, ensuring the suppression of the response from the bound [17], implies the more restrictive condition $F_{\max} = 0$, which corresponds to equilibrium where all edge currents vanish. An example where an edge current vanishes while the forces are nonzero is provided in Appendix B. They have also been shown to produce "Green-Kubo-like" fluctuation-dissipation relations [9].

Antisymmetric edge parameters.—We now calculate $\partial_{F_{nm}}\boldsymbol{\pi}$ from Equation (6). The nonzero elements of $\partial_{F_{nm}}\mathbb{K}_n$ are $\partial_{F_{nm}}W_{mn} = -W_{mn}/2$ and $\partial_{F_{nm}}W_{mm} = -\partial_{F_{nm}}W_{nm} = -W_{nm}/2$:

$$\partial_{F_{nm}}\mathbb{K}_n = \begin{array}{c} \\ 1 \\ \vdots \\ m \\ \vdots \\ N \end{array}\begin{array}{c} \begin{array}{ccccccc} 1 & \dots & n & \dots & m & \dots & N \end{array} \\ \left(\begin{array}{ccccccc} & & & & & & \\ & & & & & & \\ & & -W_{mn}/2 & & -W_{nm}/2 & & \\ & & & & & & \\ & & & & & & \end{array} \right) \end{array}. \quad (13)$$

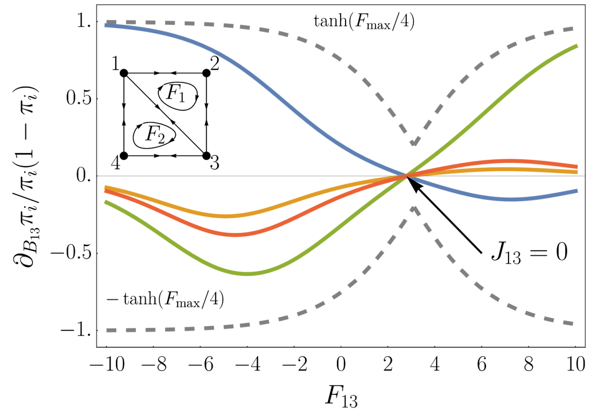

FIG. 1. Inset: example of the network with 4 states; F_1 and F_2 denote the forces in the cycles $1-2-3-1$ and $1-3-4-1$, respectively. Main: the solid curves show the responses $\partial_{B_{13}\pi_i}$ from Eq. (11) scaled to $\pi_i(1-\pi_i)$, where $i = 1, 2, 3, 4$ correspond to blue, orange, green, and red colors, respectively. In these coordinates, the dashed lines $[\pm\tanh(F_{\max}/4)]$ correspond to the bound from [17]. Black arrow indicates $J_{13} = 0$. Simulation parameters: the nondiagonal and nonzero elements of $\mathbb{W}$ are $W_{21} = 1$, $W_{31} = \mathrm{e}^{-B_{13}-F_{13}/2}$, $W_{41} = 1$, $W_{12} = 10$, $W_{32} = 1$, $W_{13} = \mathrm{e}^{-B_{13}+F_{13}/2}$, $W_{23} = 5$, $W_{43} = 10$, $W_{14} = 10$, and $W_{34} = 10$, where $B_{13} = 1$. The forces in the inset are $F_1 = F_{13} - \ln 50$, $F_2 = F_{13} - \ln 5$, which give $|F_1| = |F_2|$ at $F_{13} \approx 3.1$.

Using Eq. (6), we arrive at

$$\partial_{F_{nm}}\boldsymbol{\pi} = \mathbb{K}_n^{-1}\cdot\boldsymbol{e}_m\frac{W_{nm}\pi_m + W_{mn}\pi_n}{2} = \frac{\boldsymbol{\kappa}}{D}\frac{\tau_{nm}}{2}, \quad (14)$$

where $\tau_{nm} = W_{nm}\pi_m + W_{mn}\pi_n$ is the edge traffic (related to the expected escape rate, activity, and frenesy [29]). In Ref. [17], only the following bound was obtained $|\partial_{F_{nm}}\pi_i| \le \pi_i(1-\pi_i)$.

Responses of current and traffic.—Using Eqs. (11) and (14), the sensitivities of the edge currents read

$$\partial_{B_{nm}}\ln J_{nm} = -1 + \Delta_{nm}, \quad (15a)$$

$$\partial_{F_{nm}}\ln J_{nm} = \frac{\tau_{nm}}{J_{nm}}\frac{(1-\Delta_{nm})}{2}, \quad (15b)$$

$$\Delta_{nm} = \frac{W_{mn}\kappa_n - W_{nm}\kappa_m}{D}. \quad (15c)$$

Similarly, the sensitivities of edge traffic read

$$\partial_{B_{nm}}\ln\tau_{nm} = -1 - \frac{J_{nm}}{\tau_{nm}}\nabla_{nm}, \quad (16a)$$

$$\partial_{F_{nm}}\ln\tau_{nm} = \frac{1}{2}\left(\frac{J_{nm}}{\tau_{nm}} + \nabla_{nm}\right), \quad (16b)$$

$$\nabla_{nm} = \frac{W_{mn}\kappa_n + W_{nm}\kappa_m}{D}. \quad (16c)$$

These two results, Eqs. (15) and (16), are important because they provide explicit algebraic expressions for the response. Indeed, the variables Δ_{nm} and ∇_{nm} defined in Eqs. (15c) and (16c) do not depend on π_i. They depend only on the elements in the minors (m, n) and (m, m) of the matrix $\mathbb{K}_n$. Equations (15) and (16) depend on π_i implicitly via the current and traffic. However, J_{nm} and τ_{nm} can be defined from empirical measurements of the trajectories.

Bounds and discussion.—Another important result is that simple bounds can be obtained for Eqs. (15) and (16). They are given in Table I and bound the sensitivities $\partial_\eta \ln q$ for all combinations of $q = \{J_{nm}, \tau_{nm}\}$ and $\eta = \{B_{nm}, F_{nm}\}$. In Appendix C, we derive the following bounds for Δ_{nm} and ∇_{nm},

$$0 \le \Delta_{nm} \le 1, \tag{17a}$$

$$|\nabla_{nm}| \le \Delta_{nm} \le 1, \tag{17b}$$

which can be used to prove all bounds in Table I. Indeed, inserting Eq. (17a) into Eqs. (15a) and (15b) we get two tight bounds for the current J_{nm} in Table I. Using Eqs. (16a), (16b), and (17b), we derive two tight bounds for the traffic

$$\left| \frac{\tau_{nm}}{J_{nm}} \left(\frac{\partial \ln \tau_{nm}}{\partial B_{nm}} + 1 \right) \right| \le 1, \tag{18a}$$

$$\left| \frac{2\partial \ln \tau_{nm}}{\partial F_{nm}} - \frac{J_{nm}}{\tau_{nm}} \right| \le 1. \tag{18b}$$

The simpler bounds for τ_{nm} shown in Table I are not tight anymore. They are obtained using Eq. (17b) and $|J_{nm}/\tau_{nm}| \le 1$ in Eqs. (16a) and (16b). To discuss the saturation of the tight bounds in Table I and Eq. (18), we consider one of them:

$$-1 \le \partial_{B_{nm}} \ln J_{nm} \le 0. \tag{19}$$

The upper bound in Eq. (19) is simple to understand: a higher energy barrier (B_{nm}) always results in a lower absolute value of the current between states n and m. This bound is saturated at $\Delta_{nm} = 1$, when the current response vanishes [see Eq. (15a)]. The value of Δ_{nm} is defined by the topology of the network and the elements of the matrix $\mathbb{W}$ (kinetic parameters). By changing them, one can reduce the response of the current. Numerical simulations from Fig. 2(a) shows the existence of configurations with $\Delta_{nm} \approx 1$. To reach the lower bound in Eq. (19), one needs $\Delta_{nm} = 0$. However, in Appendix C we prove that $\Delta_{nm} = 0$ only if $W_{nm} = W_{mn} = 0$ or $\kappa_m = \kappa_n = 0$, where the former condition is equivalent to $J_{nm} = 0$. Therefore, excluding the case $\kappa_m = \kappa_n = 0$, the lower bound of Eq. (19) can be saturated only for a zero current. This is illustrated by the numerical simulations shown in Fig. 2,

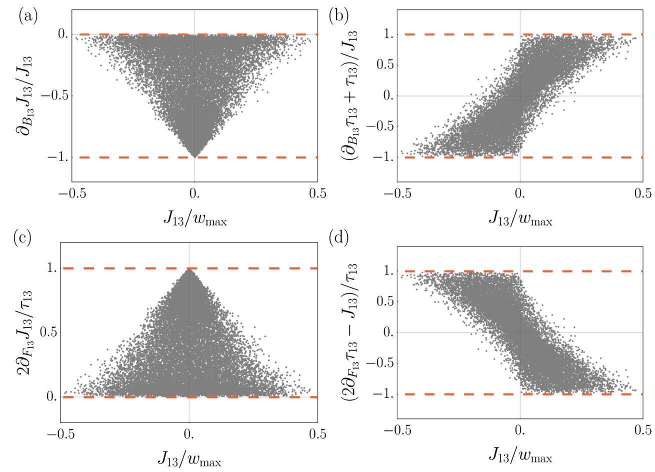

FIG. 2. (a)–(d) Illustrations of the bounds of J_{nm} from Table I and τ_{nm} from Eq. (18). The dashed lines show the corresponding bounds. The dots are the result of numerical calculations for 20 000 random matrices $\mathbb{W}$ with the elements defined by Eq. (D1). The network corresponds to the inset in Fig. 1.

where the set of possible values $\partial_{B_{nm}} \ln J_{nm}$ touches the edge -1 only at one point $J_{nm} = 0$. The bound for the sensitivity $\partial_{F_{nm}} \ln J_{nm}$ has the same properties as Eq. (19). The bounds in Eq. (18) saturate at $\nabla_{nm} = \pm 1$, which implies $\Delta_{nm} = 1$; see Eq. (17b).

Future studies.—Our first main result Eq. (6) provides a general algebraic expression of a static response with respect to any parametrization of the rate matrix. Our other results rely on the Arrhenius-like form (7) of the rates, which allows us to perturb isolated edges. This parametrization is directly relevant for instance for barrier crossing in the low noise limit, for enzymatic reactions, and for quantum dots. In these examples, the edge parameter is given, respectively, by the height of the barrier [26], the concentration of enzyme [30], or the tunneling rates [31]. Its relevance for chemically driven (e.g., via ATP hydrolysis) unimolecular chemical reaction networks is explained in Supplemental Material [32]. But our methodology can also be extended to more general rate matrices. For instance, when nonconservative forces act on multiple edges [16,27], a perturbation of the force f will imply that the matrix $\partial_f \mathbb{K}_n$ has only nonzero elements (i, j) on the edges (i, j) carrying f. Particular topologies of the rate matrix may still make analytical calculations of Eq. (6) possible. An example is the CMOS inverter of Ref. [37] described by a tridiagonal rate matrix. It could also be used to study the stationary responses of other physical observables (beyond currents and activities) [38,39], as well as to study time-dependent “Green-Kubo-Agarwal-like” relations [7,11]. We considered reversible transitions. Perturbations of B_{nm} and F_{nm} for an irreversible transition ($W_{mn} = 0$) give rise to a single nonzero element with-index (m, n) in Eqs. (10) and (13). A similar modification can be performed for systems without a local detailed balance condition, where the elements W_{ij} and W_{ji} are independent.

This research was funded by project ChemComplex (C21/MS/16356329) funded by Fonds National de la Recherche—FNR, Luxembourg. We thank Massimo Bilancioni for detailed feedback on our manuscript.

Appendix A: Derivation of Eq. (3).—We derive Eq. (3). Our strategy is to first find a solution for $\boldsymbol{\pi}$ assuming that $D \neq 0$. Then, since $\mathbb{W}$ is an irreducible rate matrix, the vector $\boldsymbol{\pi}$ is unique, and this allows us to validate our assumption. The matrix $\mathbb{K}_i$ can be transformed into $\mathbb{K}_j$ by linear operations with the rows, which preserve the determinant ($\det \mathbb{K}_i = \det \mathbb{K}_j$). To find the ith element of the vector $\boldsymbol{\pi}$, we use Cramer's rule for the matrix $\mathbb{K}_i$ in Eq. (2a), which gives us $\pi_i = (-1)^{i+i} M_{ii}(\mathbb{K}_i^\intercal)/D = M_{ii}(\mathbb{W})/D$, where $M_{ii}(\mathbb{A})$ are principal minors of order $N-1$ for the matrix $\mathbb{A}$, and where we use $M_{ii}(\mathbb{K}_i^\intercal) = M_{ii}(\mathbb{W})$. Since $\sum_{i=1}^N \pi_i = \sum_{i=1}^N M_{ii}(\mathbb{W})/D = 1$, we find that D is the sum of the principal minors of the matrix $\mathbb{W}$. On the other hand, the sum of the principal minors of $\mathbb{W}$ can be written in terms of its eigenvalues using elementary symmetric polynomials of order $N-1$ (see p. 494 in [40]):

$$D = \sum_{i=1}^{N} M_{ii}(\mathbb{W}) = \sum_{1 \le i_1 < \ldots < i_{N-1} \le N} \lambda_{i_1} \ldots \lambda_{i_{N-1}}. \tag{A1}$$

Using the fact that $\mathbb{W}$ has a single zero eigenvalue (irreducible rate matrix), the right-hand side of Eq. (A1) contains only one term, which corresponds to Eq. (3) and shows that $D \neq 0$.

Appendix B: Example of network.—In Fig. 1, we consider the responses $\partial_{B_{13}} \pi_i$ with $i = 1, \ldots, 4$, for the network given in the inset, and compare it to the bound $|\partial_{B_{nm}} \pi_i| \le \pi_i (1 - \pi_i) \tanh(F_{\max}/4)$ obtained in [17]. We see that J_{13} can vanish even at nonzero value $F_{\max} = \max(|F_1|, |F_2|) \neq 0$. In other words, the system is out of equilibrium but the edge 1–3 is detailed balanced.

Appendix C: Proof of bounds in Eq. (17).—We prove the bounds in Eq. (17). The determinant $D = \det \mathbb{K}_n$ on the mth row of the matrix $\mathbb{K}_n$ can be written as

$$\begin{aligned} D = {} & (-1)^{m+n} W_{mn} M_{mn}(\mathbb{K}_n) + (-1)^{m+m} W_{mm} M_{mm}(\mathbb{K}_n) \\ & + \sum_{i \neq m,n} (-1)^{i+m} W_{mi} M_{mi}(\mathbb{K}_n). \end{aligned} \tag{C1}$$

Using Eqs. (12) and (C1) we find an explicit dependence of D on the parameters B_{nm} and F_{nm} as follows:

$$D(B_{nm}, F_{nm}) = W_{mn}(B_{nm}, F_{nm}) \kappa_n - W_{nm}(B_{nm}, F_{nm}) \kappa_m + C, \tag{C2}$$

where C denotes the sum of all terms that do not depend on B_{nm} and F_{nm}. From Eq. (3) we have that the sign of the determinant $\operatorname{sgn} D = (-1)^{N-1}$ is fixed and does not depend on B_{nm} and F_{nm}. Using the fact that C does not depend on B_{nm}, we can determine the sign of C from Eq. (C2) in the limit $B_{nm} \to \infty$, where $W_{nm}, W_{mn} \to 0$:

$$\operatorname{sgn} C = \lim_{B_{nm} \to \infty} \operatorname{sgn} D = (-1)^{N-1}. \tag{C3}$$

Using the fact that the signs of C and $\det \mathbb{K}_n$ are the same, we can rewrite Eq. (15c) using Eq. (C2) as

$$\Delta_{nm} = 1 - \left| \frac{C}{D} \right|, \tag{C4}$$

which gives us the upper bound in Eq. (17a).

In the case $\kappa_n = 0$, $\kappa_m = 0$, Eqs. (15c) and (16c) satisfy the bounds (17a) and (17b). Considering $\kappa_n \neq 0$ and $\kappa_m \neq 0$, the following limits of Eq. (C2) hold:

$$\lim_{B_{nm} \to -\infty} \frac{W_{mn}\kappa_n - W_{nm}\kappa_m}{D} = 1, \tag{C5a}$$

$$\lim_{F_{nm} \to \infty} \frac{W_{nm}\kappa_m}{D} = -1, \tag{C5b}$$

$$\lim_{F_{nm} \to -\infty} \frac{W_{mn}\kappa_n}{D} = 1. \tag{C5c}$$

Since $\operatorname{sgn}(W_{mn}\kappa_n / \det \mathbb{K}_n)$ and $\operatorname{sgn}(W_{nm}\kappa_m / \det \mathbb{K}_n)$ are fixed, we can find them using Eqs. (C5b) and (C5c):

$$\operatorname{sgn}\left(\frac{W_{mn}\kappa_n}{\det \mathbb{K}_n} \right) = \lim_{F_{nm} \to -\infty} \frac{W_{mn}\kappa_n}{D} = 1, \tag{C6a}$$

$$\operatorname{sgn}\left(\frac{W_{nm}\kappa_m}{\det \mathbb{K}_n} \right) = \lim_{F_{nm} \to \infty} \frac{W_{nm}\kappa_m}{D} = -1. \tag{C6b}$$

Equation (15c) and (C6) imply that $\Delta_{nm} \ge 0$ that proves the lower bound in Eq. (17a). Combining this bound with Eq. (C4), we derive the inequalities (17a).

We use Eq. (C6) to write

$$\kappa_n \kappa_m < 0. \tag{C7}$$

The lower bound in Eq. (17a) is saturated only when $W_{nm} = W_{mn} = 0$, while for $W_{nm} \neq 0$ the condition in Eq. (C7) implies $\Delta_{nm} \neq 0$. The upper bound in Eq. (17a) is saturated in the limit $B_{nm} \to -\infty$ [see Eqs. (15c) and (C5a)], as well as when $C = 0$.

To find bounds for ∇_{nm}, we rewrite it as follows:

$$\nabla_{nm} = \Delta_{nm} \frac{W_{mn}\kappa_n + W_{nm}\kappa_m}{W_{mn}\kappa_n - W_{nm}\kappa_m}. \tag{C8}$$

If $W_{mn}\kappa_n = 0$, then $\nabla_{nm} = -\Delta_{nm}$, otherwise we have

$$\nabla_{nm} = \Delta_{nm}\frac{1+a}{1-a}, \quad \text{where } a = \frac{W_{nm}\kappa_m}{W_{mn}\kappa_n} \le 0. \tag{C9}$$

Since $|(1+a)/(1-a)| \le 1$ for $a \le 0$, we find Eq. (17b).

In the case $\kappa_n = 0$, $\kappa_m \neq 0$ (respectively, $\kappa_n \neq 0$, $\kappa_m = 0$), we derive Eq. (17a) using Eq. (C4) and Eq. (C6b) [respectively, Eq. (C6a)]; and we have $\nabla_{nm} = -\Delta_{nm}$ (resp. $\nabla_{nm} = \Delta_{nm}$).

Appendix D: Numerical simulations.—In Fig. 2, we numerically verify the bounds in Table I and Eq. (18) using random generated rate matrices for the network shown in the inset of Fig. 1. We generated the matrix $\mathbb{W}$ using random numbers ω_{ij} with a homogeneous distribution in the range $0 < \omega_{ij} \le \omega_{\max}$, where $\omega_{\max} = 100$. All nondiagonal elements W_{ij} with $i \neq j$ are defined as

$$W_{ij} = \begin{cases} 0, & i=2, j=4, \quad \text{and} \quad i=4, j=2, \\ \omega_{13}e^{-B_{13}+F_{13}/2}, & i=1, j=3, \\ \omega_{31}e^{-B_{13}-F_{13}/2}, & i=3, j=1, \\ \omega_{ij}, & \text{else.} \end{cases} \tag{D1}$$

To calculate the responses, we take the values F_{13} and B_{13} randomly within the range $(-r, r)$, where $r = 3$.

*Corresponding author: timur.aslyamov@uni.lu
†Corresponding author: massimiliano.esposito@uni.lu

[1] U. M. B. Marconi, A. Puglisi, L. Rondoni, and A. Vulpiani, Phys. Rep. **461**, 111 (2008).
[2] M. Polettini and M. Esposito, J. Stat. Phys. **176**, 94 (2019).
[3] J. A. Owen and J. M. Horowitz, Nat. Commun. **14**, 1280 (2023).
[4] R. Kubo, Rep. Prog. Phys. **29**, 255 (1966).
[5] D. Forastiere, R. Rao, and M. Esposito, New J. Phys. **24**, 083021 (2022).
[6] G. S. Agarwal, Z. Phys. A Hadrons Nucl. **252**, 25 (1972).
[7] U. Seifert and T. Speck, Europhys. Lett. **89**, 10007 (2010).
[8] J. Prost, J. F. Joanny, and J. M. R. Parrondo, Phys. Rev. Lett. **103**, 090601 (2009).
[9] B. Altaner, M. Polettini, and M. Esposito, Phys. Rev. Lett. **117**, 180601 (2016).
[10] M. Baiesi, C. Maes, and B. Wynants, Phys. Rev. Lett. **103**, 010602 (2009).
[11] M. Baiesi and C. Maes, New J. Phys. **15**, 013004 (2013).
[12] M. Baldovin, L. Caprini, A. Puglisi, A. Sarracino, and A. Vulpiani, in *Nonequilibrium Thermodynamics and Fluctuation Kinetics: Modern Trends and Open Questions* (Springer, New York, 2022), pp. 29–57.
[13] T. Hatano and S. I. Sasa, Phys. Rev. Lett. **86**, 3463 (2001).
[14] G. Falasco, T. Cossetto, E. Penocchio, and M. Esposito, New J. Phys. **21**, 073005 (2019).
[15] N. Shiraishi, Phys. Rev. Lett. **129**, 020602 (2022).
[16] A. Dechant and S.-i. Sasa, Proc. Natl. Acad. Sci. U.S.A. **117**, 6430 (2020).
[17] J. A. Owen, T. R. Gingrich, and J. M. Horowitz, Phys. Rev. X **10**, 011066 (2020).
[18] E. L. King and C. Altman, J. Phys. Chem. **60**, 1375 (1956).
[19] T. L. Hill, J. Theor. Biol. **10**, 442 (1966).
[20] J. Schnakenberg, Rev. Mod. Phys. **48**, 571 (1976).
[21] A. C. Barato and U. Seifert, Phys. Rev. Lett. **114**, 158101 (2015).
[22] T. R. Gingrich, J. M. Horowitz, N. Perunov, and J. L. England, Phys. Rev. Lett. **116**, 120601 (2016).
[23] G. Falasco and M. Esposito, Phys. Rev. Lett. **125**, 120604 (2020).
[24] N. G. Van Kampen, *Stochastic Processes in Physics and Chemistry* (Elsevier, New York, 1992), Vol. 1.
[25] M. Evans and R. Blythe, Physica (Amsterdam) **313A**, 110 (2002).
[26] G. Falasco and M. Esposito, Phys. Rev. E **103**, 042114 (2021).
[27] R. Rao and M. Esposito, New J. Phys. **20**, 023007 (2018).
[28] C. Maes, SciPost Phys. Lect. Notes **032** (2021).10.21468/SciPostPhysLectNotes.32
[29] C. Maes, Phys. Rep. **850**, 1 (2020).
[30] A. Wachtel, R. Rao, and M. Esposito, New J. Phys. **20**, 042002 (2018).
[31] R. Sánchez, P. Samuelsson, and P. P. Potts, Phys. Rev. Res. **1**, 033066 (2019).
[32] See Supplemental Material at http://link.aps.org/supplemental/10.1103/PhysRevLett.132.037101 for discussion of chemical application, which includes Refs. [33–36].
[33] R. Rao and M. Esposito, Phys. Rev. X **6**, 041064 (2016).
[34] J. Gunawardena, PLoS One **7**, e36321 (2012).
[35] T. Aslyamov, F. Avanzini, E. Fodor, and M. Esposito, Phys. Rev. Lett. **131**, 138301 (2023).
[36] T. Hill, *Free Energy Transduction in Biology: The Steady-State Kinetic and Thermodynamic Formalism* (Academic Press, New York, 1977).
[37] A. Gopal, M. Esposito, and N. Freitas, Phys. Rev. B **106**, 155303 (2022).
[38] G. F. Martins and J. M. Horowitz, Phys. Rev. E **108**, 044113 (2023).
[39] H.-M. Chun and J. M. Horowitz, J. Chem. Phys. **158**, 174115 (2023).
[40] C. Meyer, *Matrix Analysis and Applied Linear Algebra* (Society for Industrial and Applied Mathematics, Philadelphia, 2000).